Published in final edited form as:
Anticancer Drugs. 2013 March ; 24(3): . doi:10.1097/CAD.0b013e32835d29fd.

Dual Inhibition of AlphaV Integrins and Src Kinase Activity as A Combination Therapy Strategy for Colorectal Cancer

Jingquan Jia[1], **Alex Starodub**[2], **Ian Cushman**[3], **Yingmiao Liu**[1], **Deborah J. Marshall**[4], **Herbert I. Hurwitz**[1], and **Andrew B. Nixon**[1,*]

[1]Division of Medical Oncology, Duke University Medical Center

[2]Indiana University Health Goshen Center for Cancer Care

[3]Department of Pharmacology and Cancer Biology, Duke University Medical Center

[4]Oncology Research, Janssen Pharmaceuticals R&D

Abstract

Objective—Src and α_V integrins are both important for tumor growth and angiogenesis. They are interconnected and responsible for important features of the tumor phenotype including invasiveness, metastasis, angiogenesis and resistance to apoptosis. This study examines whether combinational inhibition of both integrin and Src pathways would exhibit greater anti-angiogenesis and anti-tumor effects than either pathway alone.

Method—Using *in vitro* cell culture systems, the activity of CNTO95 (Intetumumab), an α_V integrin inhibitor, and dasatinib, a Src inhibitor, on proliferation, adhesion and migration was evaluated in colon cancer cell lines, HCT-116 and RKO, as well as HUVEC cells. The effects of CNTO95 and dasatinib on the activation of Src and integrin pathway signal transduction were also measured by western blotting.

Results—The combination of CNTO95 plus dasatinib inhibited adhesion, migration and paxillin phosphorylation in both HCT-116 and RKO cells. CNTO95 and dasatinib also led to increased apoptosis of HCT-116 cells; however, similar effects were not observed in RKO cells. In addition, dual treatment of CNTO95 and dasatinib produced enhanced effects on HUVEC cell proliferation, invasion and paxillin phosphorylation.

Conclusion—Our results suggest that concurrent inhibition of both the integrin and src pathways elicit more pronounced anti-angiogenic and anti-tumor effects than with either pathway being inhibited alone.

Keywords

integrins; src; paxillin; FAK; colorectal cancer

Introduction

Integrins are a diverse family of cell-surface heterodimeric proteins that mediate interactions between cells and the extracellular matrix (ECM) as well as cell-cell interactions[1]. Each integrin, consisting of a large α subunit and a smaller β subunit, serves as a receptor for

*Correspondence to: Andrew Nixon, Division of Medical Oncology, Duke University Medical Center, Box 2631, Durham, NC 27710., anixon@duke.edu.
Note: J. Jia and A. Starodub contributed equally to this work

Conflicts of Interest: For the remaining authors, no conflicts of interest are declared.

various ECM ligands, soluble ligands, and other cell surface ligands[2]. Integrins and their ligands play key roles in regulating cell survival, proliferation, adhesion and migration[3-5]. In addition to mediating cell adhesion, integrins relay molecular cues from the cellular environment to the cytoskeleton through the activation of multiple intracellular signaling pathways[6]. Upon ligand binding, signaling cascades are initiated through recruitment and activation of Src kinase via phosphorylation of focal adhesion kinase (FAK). The activated FAK-Src complex then activates a series of downstream events that are essential for many physiological and pathological functions of integrins[7].

The α_V integrin subfamily is composed of 5 receptors: $\alpha_V\beta1$, $\alpha_V\beta3$, $\alpha_V\beta5$, $\alpha_V\beta6$, and $\alpha_V\beta8$[8] The α_V integrins have been implicated in tumor angiogenesis and tumor progression[9, 10] and integrin overexpression has been observed in various types of human cancers [11-17]. CNTO95 (Intetumumab) is a fully humanized, monoclonal antibody that binds to and blocks human α_V integrins[18]. In preclinical studies, CNTO95 not only exhibited potent anti-angiogenic activity in nude rat models, due to its cross reactivity with rat integrins[18], but also inhibited tumor growth and metastasis in both nude rats and nude mice[18, 19]. CNTO95 has been evaluated in several early phase clinical trials across a range of tumor types. Multiple phase I trials found CNTO95 to be safe and well tolerated in patients with advanced solid tumors [20-22]. In addition, the combination of darcabazine plus CNTO95 in stage IV melanoma patients exhibited a nonsignificant trend towards improved overall survival [23].

Src is a small non-receptor tyrosine kinase that belongs to the Src family kinases (SFKs) [24]. SFKs regulate diverse cellular functions including proliferation, migration, cytoskeletal reorganization, and cellular survival by interacting with and/or phosphorylating specific substrates[25]. Src is over-expressed and/or activated in a wide range of tumors including human colon and rectal adenocarcinomas[26]. Notably, colorectal cancers show a progressive increase in Src expression levels and Src activity as the tumor stage advances, suggesting a potential role for Src in assisting tumor progression[27]. Dasatinib is a small molecule inhibitor of Src kinase activity, but also inhibits other tyrosine kinases such as Abl, c-kit and PDGFR-β[28]. It has been approved for use in chronic myeloid leukemia (CML), resistant or intolerant to imatinib and is currently in clinical trials for use in other tumor types[29].

Due to the upregulation of α_V integrins and the activation of Src in colorectal cancer cells, the potential for cooperative or synergistic interactions exist. Importantly, while the activation of Src and α_V integrins can occur independently of each other, they later converge to form a stable FAK-Src complex, which is important for cell invasion and metastasis[30]. To explore whether dual inhibition of α_V integrins and Src kinase activity could potentially be a more effective anti-tumor strategy, we examined the effects of CNTO95 and dasatinib on human colon cancer cell proliferation, adhesion and migration *in vitro*. In addition, we investigated the proliferation, migration, and tubular formation of human endothelial cells in response to dual inhibition regimen *in vitro*, as an indication of its anti-angiogenic activity. Lastly, to better understand the underlying molecular mechanisms of CNTO95 and dasatinib treatment, we further evaluated the downstream signaling events.

Materials and Methods

Cell culture

HCT-116 and RKO cells were obtained from the American Type Culture Cell Collection through the Duke Cell Culture Facility. HUVEC cells were purchased from Clonetics through Duke Cell Culture Facility. Cell lines were passaged for fewer than 6 months. HCT-116 and RKO cell lines were authenticated by the cell bank using short tandem repeat

PCR and HUVEC cell line was characterized in accordance with Clonetics test procedures and sampling plans. All cells were sterile and confirmed to be free of mycoplasma. HCT-116 cells were cultured in McCoy's 5a medium containing 10% FBS, 2mM L-glutamine and 1% penicillin-streptomycin. RKO cells were cultured in Eagle's Minimum Essential Medium (EMEM) supplemented with 10% FBS, 1% penicillin-streptomycin, 2mM L-glutamine and Eagle's BSS. HUVEC cells were cultured in complete Endothelial Basal Medium-2 (EBM-2) from Clonetics supplemented with EGM-2 MV BulletKit (Lonza, Cat# CC-3162). All cells were maintained at 37°C in the presence of 5% CO_2.

Flow Cytometry

Integrin staining—Briefly, cells were passaged 24 hr prior to analysis. Cells were harvested in Versene + 0.1% sodium azide (w/v) and washed with DPBS + 0.1% sodium azide (w/v), resuspended in FACS buffer (PBS + 2% BSA + 0.1% sodium azide) at 2.5×10^6 cells/ml. Cells were stained with 15μg/ml primary antibody for 45 min on ice, washed twice and then stained with secondary antibody at 10μg/ml on ice in the dark. Cells were resuspended in 500μl FACS buffer and analyzed on a FACS Canto (BD Biosciences) flow cytometer and Flowjo software (Tree Star Inc.).

Cell proliferation and viability: 5×10^6 cells were labeled with 1μM Carboxyfluorescein succinimidyl ester (CFSE; eBioscience, Cat# 65-0850) and plated onto vitronectin-coated plates (Calbiochem, cat#681105). Cells were cultured overnight before the addition of CNTO95 or dasatinib, and then grown for 24 hr. Cells were harvested with 0.05% Trypsin-EDTA and stained with APC- conjugated Annexin V (eBioscience, Cat# 88-8007) and 7AAD (eBioscience, Cat# 00-6993).

Preparation of cell lysates and Western blotting

Tissue culture dishes were coated with 1μg/ml human vitronectin overnight at 4°C and subsequently blocked with 1% BSA for 2 hr at room temperature. Cells were then plated and incubated overnight at 37°C in the presence of 5% CO_2. Culture media was removed and replaced with serum-free media containing drug or vehicle for 2 hr. The serum-free media was then removed and replaced with complete medium containing drug or vehicle for 20 min. Cell lysates were prepared with a modified RIPA buffer containing 20mM HEPES, 154mM NaCl, 2mM $MgCl_2$, 1mM EDTA, 1mM EGTA, 1% Triton X-100, proteinase inhibitor cocktail (Roche, cat# 04693150001) and phosphatase inhibitor cocktails I and II (Sigma, cat# P2850 and P5726). Lysates were centrifuged at 16,000×g at 4°C to remove unbroken cells, nuclei and other particulates. Proteins were separated on 4-12% NuPAGE gels, transferred to nitrocellulose membranes for Western analysis. Images were acquired and quantified using the Odyssey Infrared Imaging System (Licor Biosciences).

Antibodies

Antibodies used for flow cytometry are: mouse IgG_1 anti-Human Integrin α_V monoclonal antibody (Millipore International, cat# MAB1953Z), mouse IgG_1 anti-Human Integrin $\alpha_V\beta3$ [CD51/61] monoclonal antibody (Millipore International, cat# MAB1976Z), mouse IgG_1 anti-Human Integrin $\alpha_V\beta5$ monoclonal antibody (Millipore International, cat# MAB1961Z), mouse IgG_{2a} anti-Human Integrin $\alpha_V\beta6$ monoclonal antibody (Millipore International, cat# MAB2077Z), mouse IgG_1 anti-Human Integrin β1 monoclonal antibody (Millipore international, cat# MAB1951Z), mouse IgG_1 Isotype Control (BD Biosciences. cat# 557273), mouse IgG_{2a} Isotype Control (BD Biosciences, cat# 554126), FITC-conjugated AffiniPure $F(ab')_2$ Fragement Goat Anti-Human IgG, Fc_γ (Jackson ImmunoResearch Laboratories, cat# 109-096-098), FITC-conjugated AffiniPure $F(ab')_2$ Fragement Goat Anti-Mouse IgG, (H+L) (Jackson ImmunoResearch Laboratories, cat# 115-096-003). CNTO95

and F105 (human monoclonal antibody, IgG_1) isotype controls were generously provided by Janssen Pharmaceutical R&D.

Antibodies used for western blotting are: anti-total FAK (cat#3285), anti phospho FAK Y397 (Millipore, MAB1144), anti-phospho FAK Y576/577 (cat#3281), anti-phospho FAK 925 (cat#3284), anti-total paxillin (cat#2542), anti-phspho paxillin Y118 (cat#2541), anti-total Src (cat#2108), anti-phospho Src Y416 (cat#2113), anti-β actin (Sigma, cat#A5441). Above antibodies were purchased from Cell Signaling Technology except noted otherwise.

Secondary antibodies include Goat anti-rabbit 680 (Invitrogen, cat#A21109), Goat anti-mouse 680 (Invitrogen cat#A21058) and Goat anti-mouse 800 (VWR, cat#610-132-121)

Cell Viability Assay

Cell viability was determined using MTS assays from Promega (Madison, WI) according to the manufacturer's instruction. Briefly, cells were plated in triplicate in 96-well plates coated with vitronectin and blocked with BSA at a density of 50,000 cells per well. Cells were incubated for 16 h before the addition of CNTO95 or dasatinib, and then allowed to grow for 24 hr. The MTS substrate was added and the OD490 was determined 2 hr later.

Cell Adhesion Assay

Cells were washed with PBS, incubated in CellStripper™ (Cellgro), and resuspended in media. Excess Cellstripper™ was removed by brief centrifugation (1000×g for 5 min). HCT-116 (40,000 cells/well) or RKO (50,000 cells/well) cells were dispensed into 96-well plates coated with vitronectin (5 ug/ml) and allowed to adhere overnight. The following day, cells were treated for 4 hr with the indicated amounts of CNTO95 in the absence or presence of 10 nM dasatinib. Non-adherent cells were removed; the remaining cells were then fixed and stained with crystal violet. Crystal violet was eluted with methanol and adherent cells were quantitated at 550 nm. After background subtraction, data points were normalized to DMSO (control) treated wells and plotted as percent control.

Focal Adhesion Staining

Cells (15,000/coverslip) were plated on coverslips coated with 5 mg/ml vitronectin and fixed 48 hr later in 4% paraformaldehyde. The cells were permeabilized with 0.1% Triton X-100, incubated with an anti-vinculin monoclonal antibody (Sigma), followed by incubation with a Cy3-conjugated anti-mouse secondary antibody (Jackson Labs). The coverslips were washed and affixed to slides with mounting media containing DAPI (Molecular Probes) to visualize nuclei. Images were obtained with a Zeiss Axio Imager fluorescence microscope equipped with a digital camera and Metamorph software.

Cell Migration Assays

Cell invasion and migration assays were performed using the BD Biocoat Angiogenesis System (BD Bioscience), according to the manufacturer's protocol. Briefly, 2.5×10^4 cells were added to the top chamber, HUVECs were incubated for 15 hr at 37°C while cancer cells were incubated for 24 hr at 37°C. In both cases, at the end of incubation period, the top chambers were transferred to the PBS containing wells. The inserts were processed by wiping out cells from the inside of the top chamber using cotton swabs. The cells on the outer surface of the insert were stained using the 3-step stain set (Richard-Allen Scientific). The inserts were removed from the frame and mounted under a cover slide with Cytoseal-60 (Richard-Allen Scientific). The cells occupying a strip were visualized using a Nikon microscope (200× magnification) and counted. The counts obtained in randomly selected two perpendicular diameters were averaged.

HUVEC tubular network formation

HUVEC were pre-treated with CNTO95, dasatinib or both drugs for 8 hours. The cells were harvested and maintained in drug containing medium, and 1.5×10^4 HUVEC were inoculated onto pre-polymerized ECMatrix gel (*In vitro* angiogenesis assay kit, Chemicon, Temecula, CA). After overnight incubation, cells were visualized using an Axio Observer microscope (Carl Zeiss Microscopy Ltd) at the Duke University Light Microscopy Core Facility. Closed polygons were counted; total number of tubes and total tube length were measured using MetaMorph software.

Software and statistical analysis

Flow cytometry data were analyzed by Flowjo 8.8.6 (Tree Star, Inc.). Western data were analyzed using the Odyssey 3.0 system (LiCor Biosciences). Graphs were generated using Prism 5 software (GraphPad Software). The statistical differences between the single agent treatment and control were evaluated by Student's t test. The statistical differences between the combinatorial treatments compared to single agent treatments were evaluated by one-way ANOVA followed by Bonferroni's multiple comparison tests.

Results

Multiple colon cancer cell lines were initially tested for sensitivity to CNTO95-induced growth inhibition, as determined by MTS assays. Cell lines exhibiting greater than 15% growth inhibition at 1 ug/ml CNTO95 were designated as sensitive cell lines (HCT-116, HCT15, SW48, SW403, and DLD-1), and cell lines exhibiting less than 15% growth inhibition at 1 ug/ml CNTO95 were designated as resistant cell lines (RKO, WiDr, Colo320, SW1417, SW1463, and HT-29). When compared, the sensitive vs. resistant groups were found to be significantly different from one another (unpaired T test; p=0.0148). Of all cell lines tested, HCT-116 cells were the most sensitive to CNTO95 (46.0% growth inhibition) while RKO cells were among the most resistant to CNTO95 (10.9% growth inhibition). Additionally, both cell lines exhibited good growth characteristics *in vitro*. For those reasons, HCT-116 and RKO cell lines were chosen as representative “sensitive” and “resistant” cell lines to next explore the effect(s) of combining CNTO95 and dasatinib across a spectrum of cellular and molecular readouts.

Human colon cancer cell lines express multiple α_V integrins

The expression patterns of α_V integrins on HCT-116 and RKO cells were determined by flow cytometry and expression levels were assessed by mean fluorescence intensity. As shown in Fig. 1, the level of α_V expression in HCT-116 cells is nearly five fold greater that what was observed in RKO cells. In particular, $\alpha_V\beta5$ expression is two times greater in HCT-116 cells compared to RKO cells. Also, $\alpha_V\beta6$ expression is readily detectable in HCT-116 cells, whereas RKO cells were essentially negative for $\alpha_V\beta6$ staining. Neither HCT-116 nor RKO cells express $\alpha_V\beta3$. Little or no $\beta1$ expression was seen in either cell type, indicating that $\alpha_V\beta1$ integrins were not expressed to appreciable levels in these cells. HCT-116 and RKO cells were positively stained by CNTO95, but not the isotype control, confirming the specific binding of CNTO95 to these cells through α_V integrins. Consistent with the α_V integrin expression pattern, CNTO95 staining on HCT-116 cells was three fold greater than that observed on RKO cells.

Combination of CNTO95 and dasatinib on cell viability of human colon cancer cell lines

The combinatorial effect(s) of CNTO95 and dasatinib on the growth of HCT-116 cells and RKO cells was determined using MTS assays. Dasatinib treatment (24 hr) of HCT-116 cells led to a dose-dependent decrease in viability, with the maximum inhibition reached at 25nM

(Fig. 2A). CNTO95 (10ug/ml; 24 hrs) alone reduced the number of viable HCT-116 cells by about 20%. The addition of CNTO95 to dasatinib-treated HCT-116 cells led to an additional 10-20% inhibition compared to dasatinib alone (Fig. 2A). In contrast, RKO cells exhibited little to no change in overall viability after exposure to either 10ug/ml CNTO95 or various doses of dasatinib for 24 hr (Fig. 2B). Dasatinib is known to inhibit multiple tyrosine kinases at nanomolar concentrations; however, even when exposed to 200nM of dasatinib, RKO cell viability was unaffected.

While MTS assays measure overall cell viability, we wanted to differentiate between cell death and cell proliferation, both of which contribute to the amount of viable cells. In order to separate the effects of CNTO95 with or without dasatinib on these two cellular aspects, we tracked cell proliferation using CFSE stains and measured cell death using annexin V and 7AAD stains by flow cytometry. The intensity of CFSE fluorescence did not significantly change upon drug treatment, in either HCT-116 or RKO cells (Fig. 2C), suggesting that the proliferation of both cell types was unaffected by CNTO95 and dasatinib, alone or in combination. Next, we evaluated cell death by quantifying the percentage of annexin V positive cells (apoptotic) and 7AAD positive cells (necrotic) in both cell types. In contrast to RKO cells, apoptotic and necrotic cell death were dramatically increased in HCT-116 cells treated either with drug alone or in combination (Fig 2E, F, G, H). The combination of both drugs induced more cell death than either drug alone in HCT-116 cells (Fig 2F). It appears that both CNTO95 and dasatinib, either as single agents or in combination, limit the expansion of HCT-116 cells *in vitro* primarily by inducing apoptotic and necrotic cell death, yet have little effect on proliferation. In contrast, the proliferation and survival of RKO cells remain largely unaffected by these agents.

Combination of CNTO95 and dasatinib on serum-induced migration of human colon cancer cell lines

Cell migration is a critical process mediating tumor metastasis. CNTO95 is able to block α_V integrins, which disrupts the connection between the α_V integrins and their ECM ligands, thereby affecting tumor cell migration and metastasis. The effect of CNTO95 and dasatinib on the migration of HCT-116 cells and RKO cell was examined. As shown in Fig 3, the ability of HCT-116 cells to migrate towards serum was greatly impaired by either CNTO95 (Fig. 3A) or dasatinib (Fig. 3B) in dose dependant manners. The migration of HCT-116 cells was reduced nearly 50% by either10ng/ml CNTO95 or 5nM dasatinib (Fig. 3A,B). In comparison to either agent alone, the combination of 30ng/ml CNTO95 and 5nM dasatinib nearly abolished HCT-116 cell migration (Fig. 3C). However, much higher concentrations of CNTO95 and dasatinib were required to inhibit serum-induced migration of RKO cells (Fig. 3D,E). Even at doses as high as 3000ng/ml CNTO95 or 100nM dasatinib, RKO cells still retained 30-50% migration (Fig. 3D,E). It should be noted that at these higher doses, the combination of dasatinib and CNTO95 did inhibit RKO migration more than either drug alone. These results suggest that alternate mechanisms may support the migratory activity of RKO cells. Overall, our findings demonstrate that the migration of HCT-116 cells is sensitive to both CNTO95 and dasatinib whereas RKO cells are more resistant. Additionally, the migration of both HCT-116 and RKO cells are inhibited more by the combination of both drugs than by either drug alone.

Combination of CNTO95 and dasatinib on adhesion of human colon cancer cell lines

α_V integrins are known receptors for ECM proteins such as vitronectin and fibronectin. We tested the ability of CNTO95 to inhibit cell binding to vitronectin and whether this effect could be augmented by dasatinib. The adhesion of both HCT-116 cells and RKO cells was greatly disrupted by CNTO95 in a dose-dependent manner and the addition of 10 nM dasatinib further reduced the number of adhered cells (Fig. 4A, B). CNTO95 (0.1ug/ml)

alone inhibited HCT-116 adhesion to vitronectin by 25%, and the addition of 10 nM dasatinib augmented this effect yielding only 50% adherent cells (Fig. 4A). The adhesion of RKO cells to vitronectin was reduced by 50% upon treatment with 0.1ug/ml of CNTO95. The addition of dasatinib further decreased the number of adherent cells to about 15% (Fig. 4B).

Our observation that the adhesion of RKO cells was more easily disrupted than that of HCT-116 cells led us to postulate that the quantity and/or size of the focal adhesions are intrinsically different between the two cell lines. Indeed, vinculin staining revealed that HCT-116 cells not only had more focal adhesions, but that these focal adhesions were also intrinsically larger in size compared to the focal adhesions in the RKO cells (Fig. 4C, D).

Combination of CNTO95 and dasatinib inhibits the phosphorylation of FAK, paxillin and Src induced by serum stimulation in human colon cancer cells

Integrin engagement induces the autophosphorylation of the non-receptor tyrosine kinase FAK at Y397, creating a high affinity-binding site for Src. Once bound, Src undergoes conformation changes facilitating additional trans-phosphorylation of FAK at Y576, Y577 and Y925 by Src. The fully activated FAK-Src complex is required for the maximal activation of many substrates, including the downstream kinase, paxillin. The environmental cues are sensed by integrins, transduced by FAK and Src, and lead to eventual changes in cell mobility[31].

In order to better understand the signaling mechanism(s) affected by CNTO95 and dasatinib, we examined the effects of these agents on the phosphorylation status of FAK, Src and paxillin upon serum stimulation. As expected, dasatinib treatment of HCT-116 and RKO cells inhibited serum-induced Src phosphorylation (Fig 5A,C). In addition, dasatinib also reduced FAK phosphorylation at Y576/577 and Y925 in both cell lines, but the autophosphorylation site Y397 was largely unaffected. In contrast to dasatinib, CNTO95 treatment alone appeared to have little or no effect on the activation of FAK or Src; however, paxillin phosphorylation was inhibited in both HCT-116 and RKO cells (Fig. 5A,C). The phosphorylation of paxillin was inhibited more by combining CNTO95 and dasatinib (Fig. 5B,D) than using either drug alone, suggesting that paxillin may act as a molecular integrator that accounts for cell survival, adhesion and migration.

Combination of CNTO95 and dasatinib inhibits HUVEC proliferation, migration and integrin signal transduction

Integrins are the principle adhesion receptors used by endothelial cells to interact with their extracellular environment[9]. $\alpha_V\beta3$ and $\alpha_V\beta5$ are critical during tumor angiogenesis[32] and studies have shown that anti-α_V antagonists exhibit clear anti-angiogenic activity[18, 33]. To further investigate the effects of CNTO95 and dasatinib on endothelial cells, we used HUVEC cells as a model system. Dasatinib inhibited HUVEC cell viability in a dose-dependent manner. CNTO95 (10ug/ml) reduced viable HUVEC cells by about 20%, but the combination of CNTO95 and dasatinib elicited a much greater effect on HUVEC viability in comparison to either treatment alone at the doses tested (Fig. 6A).

Individually, CNTO95 and dasatinib were able to inhibit serum-induced migration of HUVEC cells, but when combined together, more pronounced inhibition of HUVEC migration was observed (Fig. 6B). In fact, 10ug/ml of CNTO95 plus 100nM dasatinib almost completely blocked the migration of HUVEC cells. Taken together, these results suggest that the combination of CNTO95 and dasatinib may affect tumor angiogenesis in addition to direct effects on tumor cells.

Lastly, protein lysates were extracted from drug-treated HUVEC cells after serum stimulation to examine the phosphorylation status of FAK, paxillin and Src. Although the overall signal was low, the phosphorylation of Src was diminished in the presence of dasatinib, as was the phosphorylation of FAK at Y576/577 and Y925, presumably due to the significant decrease of Src activity. Similar to our observations above using colon cancer cells, paxillin phosphorylation was also reduced, most likely as a result of compromised FAK and Src activation. CNTO95 alone had very little effect on the phosphorylation of FAK, Src and paxillin (Fig 6C). However, when CNTO95 was combined with dasatinib, increased inhibition of paxillin phosphorylation was observed (Fig. 6D). While not as pronounced, this effect was observed in both endothelial cells and colon cancer cells, suggesting that the CNTO95 and dasatinib combination may impact both the tumor directly as well as the supporting vasculature.

Combination of CNTO95 and dasatinib inhibits HUVEC tubular network formation

Capillary tube formation is an essential event during angiogenesis. It is a multi-step process involving endothelial cell adhesion, migration, differentiation and proliferation [34]. To test the effects of CNTO95 and dasatinib on angiogenesis, we utilized an *in vitro* 2-D extracellular matrix gel system to examine HUVEC tube formation. For analysis, we were able to quantify multiple endpoints, including the number of closed polygons, the number of tubes and the total length of tubes. When HUVECs were treated with 10ug/ml CNTO95 or 25nM dasatinib alone, a 10∼20% and 37∼55% reduction, respectively, in tubular network formation was noted. In addition, the combination of CNTO95 and dasatinib elicted more profound inhibition on angiogenesis, as evidenced by a 50∼65% reduction in tube formation (Fig 7A-C). When compared to HUVECs treated with either drug alone, the number of tubes and the total length of tubes were significantly lower in cells treated with the combination of both CNTO95 and dasatinib (Fig 7B,C). The combination regimen also led to significantly fewer polygons in HUVECs than CNTO95 alone. A non-significant trend was noted for less polygon formation in comparison to dasatinib treatment alone (Fig 7A). Overall, our data indicates that both CNTO95 and dasatinib blocked endothelial cell tubular network formation, while the combination of both drugs achieved a more profound inhibition.

Discussion

Anti-cancer therapeutics targeting α_V integrins have been under active development over the recent years. Among them, CNTO95 and etaracizumab are monoclonal antibodies against αVβ3 and αVβ5[35]. Others include cilengitide[36], a synthetic peptide containing RGD sequence, peptidomimetics S137 and S247[37], as well as a non-peptide antagonist PSK1404[38]. CNTO95 and cilengitide are the frontrunners that have moved to various phases of clinical trials, while S137, S247 and PSK 1404 currently remain in preclinical development. Previously, some work has been done to investigate the potential for CNTO95 to be a part of a combinational anti-cancer regimen. It has been found that CNTO95 potentiates the efficacy of fractionated radiation therapy in mouse xenograft tumor models[39]. Further, a phase I study in patients with castrate-resistant metastatic prostate cancer found that CNTO95 in combination with docetaxel and prednisone was generally safe and well tolerated[21]. The safety and efficacy of CNTO95 in combination with dacarbazine was also evaluated in a randomized phase II trial in stage IV melanoma[23]. Our study is the first to date demonstrating that dual inhibition of α_V integrins and Src kinase activity results in profound inhibition of cell survival, adhesion, migration and integrin signal transduction of both human colon cancer cells and endothelial cells *in vitro*. The inhibitory effects conferred by CNTO95 and dasatinib as a combination regimen were greater than by either drug alone, implicating CNTO95 and dasatinib as a potential

promising combined targeted therapy that possesses both anti-tumor and anti-angiogenic effects.

The expression and function of integrins in endothelial cells are well understood. In contrast, integrin expression in colon cancer cell lines has not been extensively characterized. It has been shown that RKO cells express α6β1 and α2β1 but not α6β4 [40]. However, little is known about αV expression profile of RKO cells. Our data not only demonstrate the presence of αV integrins, but also analyzed the expression pattern of various αV integrins on the surface of RKO cells in comparison to HCT116 cells. In agreement with previous work[41] we found that HCT116 cells express αVβ5 but not αVβ3. We also identified αVβ6 was expressed on HCT116 cells. In our analysis, neither RKO cells nor HCT116 cells exhibited discernible levels of β1 expression, which had been previously shown to be positive on HCT116 cells[41]. This discrepancy could be explained by the specificity of the antibodies used. Nonetheless, the characterization αV integrin expression provided a structural basis to better understand the effects of CNTO95 on the two colon cancer cell lines evaluated here.

In an effort to address whether the sensitivity or resistance to CNTO95 is determined by any genetic differences, we took bioinformatics approach to examine integrin pathway components for differential expression patterns across the 11 cell lines initially tested. Except for WiDr cell line, data regarding the other 10 cell lines are available in the Novartis/Broad CCLE public database for expression values (Affymetrix U133 +2). The average FAK expression from four unique probes is significantly higher in the resistant cell lines ($p=0.027$, data not shown). However, no statistical differences were found in αV, β3, β5, β6, src or paxillin expression between the sensitive and resistant groups. The expression of focal adhesion linker proteins, including vinculin, talin and zyxin, and the focal adhesion disassembly protease calpain were also examined; no significant differences were observed across the sensitive and resistant cell types (data not shown). These findings from our bioinformatics study suggested that sensitivity to CNTO95 treatment might be determined by the activation status of signaling proteins rather than the quantitative differences in members of the integrin pathway.

CNTO95 and dasatinib exhibited more pronounced effects on the inhibition of cell proliferation and migration of HCT-116 cells compared to RKO cells. In support of these findings, a recent study has demonstrated that $\alpha_V\beta3$ integrin and c-Src can work together as an oncogenic unit to promote anchorage-independent cell growth and metastasis of pancreatic tumor cells[42]. The viability of RKO cells, however, was not affected by CNTO95 and dasatinib either as single agents or in combination. Our results also show that the migration of RKO cells is resistant to CNTO95 and dasatinib treatment. Low concentrations of CNTO95 and dasatinib were sufficient to inhibit cell migration in HCT-116, while 20-fold higher concentrations were needed to achieve a comparable degree of inhibition in RKO cells. These findings indicate that individual human colon cancer cell lines exhibit differential dependence on α_V integrin and Src kinase activity for their survival and migration. The differing sensitivities to CNTO95 between the two cell lines may be, in part, explained by the quantitative differences in their α_V integrin expression, which leads to differential binding affinity for CNTO95 to unique cell types and subsequent signaling activation. Interestingly, further examination of the integrin signaling pathways revealed that signaling in HCT-116 and RKO cells was perturbed to a similar extend by CNTO95 and dasatinib, despite the drastic differences in their proliferation and migration behavior upon drug treatment. It is known that integrin activation elicits extensive crosstalk between multiple pathways through a complex signaling network[43]. For example, engagement of integrins induces trans-activation of growth factor receptors, such as PDGFR and EGFR[44]. Other signaling pathways that can be activated by integrins include MAPK

pathway, PI3/Akt pathway, NF-κB pathway, as well as small GTPases[45]. These intersecting signaling cascades work coordinately to regulate cell proliferation, adhesion and migration. Therefore, a more thorough examination of multiple signaling pathways may be required to help to identify key signal transduction points underlying the differential responses to CNTO95.

CNTO95 and dasatinib are effective in decreasing the adhesion of both HCT-116 and RKO cells. Focal adhesion complex formation and focal adhesion disassembly/turnover are two distinct, yet carefully orchestrated processes that mediate cell adhesion and migration. The differences in the expression of the key components involved in these two processes may be responsible for the different responses to CNTO95 and dasatinib in adhesion versus migration. A preliminary bioinformatics analysis using Novartis/Broad CCLE public database revealed higher RNA expression of FAK and zyxin, lower RNA expression of talin and calpain in RKO cells than in HCT-116 cells (data not shown). However, this analysis needs further validation of protein expression.

FAK undergoes autophosphorylation at Y397 upon integrin clustering mediated cell adhesion. Recently, Chen *et al.* demonstrated that CNTO95 treatment induced time-dependent dephosphorylation at the Y397 site in breast cancer cells[19]. However, in our system, phosphorylation of Y397 seemed to be unaffected by CNTO95. It should be noted that our analysis is different from the work done by Chen *et al.*[19] in several ways: 1) we evaluated colon cancer and endothelial cells whereas their experiments were done in breast cancer cells; 2) we measured the effect of drug treatment on Y397 phosphorylation upon serum stimulation whereas they looked at changes in the level of Y397 phosphorylation under serum-free conditions; 3) in our system, drug exposure was concurrent with starvation whereas in their system drug treatment was not initiated until cells had been starved for 2 hrs in serum free medium. Therefore, the discrepancy in the effect of CNTO95 on Y397 phosphorylation status could be due to the intrinsic differences of cell lines, the effect of serum stimulation, or the timing of drug treatment relative to cell starvation. It should be noted that the phosphorylation of two additional downstream sites, Y576 and Y925, were not significantly inhibited by CNTO95 treatment in our analysis. Moreover, the phosphorylation profile of FAK Y397, Y576 and Y925 remained consistent in HCT-116 and RKO cells, as well as in HUVEC cells, demonstrating the overall consistency within our experimental system. We also verified the specificity of all three FAK antibodies FAK Y397, Y576 and Y925 by pervanadate (to induce phosphorylation) or phosphatase (to induce dephosphorylation) treatment of cell lysates (data not shown). All phospho-FAK antibodies tested in our analysis were selective for each phospho-specific site. Nonetheless, the fact that CNTO95 was able to inhibit cell proliferation, adhesion and migration on its own clearly indicated its biological activity.

Our analysis of integrin signaling supports the view that paxillin is a potential cellular integrator of α_V integrins and Src. Dual inhibition of α_V integrins and Src reduced paxillin activation more than either agent alone. This result is consistent with the notion that both Src and FAK activity are required for the maximum activation of paxillin[46]. Paxillin has been recognized as an important adaptor protein, facilitating the interactions between proteins within the focal adhesion complex, thus playing a central role in the signal transduction of integrins upon their engagement by ECM ligands[47]. In our system, inhibition of paxillin activity closely correlated with inhibition on cell adhesion and migration. We postulate that paxillin could act as a molecular focus that integrates the combined inhibitory effects observed with CNTO95 and dasatinib.

In conclusion, our study demonstrates that the combined inhibitory effect of CNTO95 and dasatinib in both colon cancer and endothelial cells *in vitro*, suggesting additive/synergistic

anti-tumor activity *in vivo*, where both host endothelial cells and neoplastic epithelial cells contribute to tumor growth and metastasis.

Acknowledgments

The authors are grateful to Dr. Mike Gatza for his help with bioinformatics analysis. The authors would also like to thank staff of the Flow Cytometry Shared Resources at Duke Cancer Institute for their assistance.

Source of Funding: Andrew Nixon has received grant funding (#159193) from Centocor Research & Development, Inc. (now Janssen Pharmaceuticals). Herbert Hurwitz has received funding from Centocor Research & Development, Inc. (now Janssen Pharmaceuticals) and from NIH (K24-CA113755-01A1, PI: Hurwitz). Deborah Marshall is an employee of Janssen Pharmaceuticals.

Grant Support: This work was supported by Janssen Pharmaceutical R&D.

References

1. van der Flier A, Sonnenberg A. Function and interactions of integrins. Cell Tissue Res. 2001; 305:285–98. [PubMed: 11572082]
2. Plow EF, Haas TA, Zhang L, Loftus J, Smith JW. Ligand binding to integrins. J Biol Chem. 2000; 275:21785–8. [PubMed: 10801897]
3. Stupack DG, Cheresh DA. Get a ligand, get a life: integrins, signaling and cell survival. J Cell Sci. 2002; 115:3729–38. [PubMed: 12235283]
4. Schuppan D, Ocker M. Integrin-mediated control of cell growth. Hepatology. 2003; 38:289–91. [PubMed: 12883471]
5. Hood JD, Cheresh DA. Role of integrins in cell invasion and migration. Nat Rev Cancer. 2002; 2:91–100. [PubMed: 12635172]
6. Hynes RO. Integrins: bidirectional, allosteric signaling machines. Cell. 2002; 110:673–87. [PubMed: 12297042]
7. Guo W, Giancotti FG. Integrin signalling during tumour progression. Nat Rev Mol Cell Biol. 2004; 5:816–26. [PubMed: 15459662]
8. Nemeth JA, Nakada MT, Trikha M, Lang Z, Gordon MS, Jayson GC. Alpha-v integrins as therapeutic targets in oncology. Cancer Invest. 2007; 25:632–46. [PubMed: 18027153]
9. Stupack DG, Cheresh DA. Integrins and angiogenesis. Curr Top Dev Biol. 2004; 64:207–38. [PubMed: 15563949]
10. Jin H, Varner J. Integrins: roles in cancer development and as treatment targets. Br J Cancer. 2004; 90:561–5. [PubMed: 14760364]
11. Kageshita T, Hamby CV, Hirai S, Kimura T, Ono T, Ferrone S. Differential clinical significance of alpha(v)Beta(3) expression in primary lesions of acral lentiginous melanoma and of other melanoma histotypes. Int J Cancer. 2000; 89:153–9. [PubMed: 10754493]
12. Arihiro K, Kaneko M, Fujii S, Inai K, Yokosaki Y. Significance of alpha 9 beta 1 and alpha v beta 6 integrin expression in breast carcinoma. Breast Cancer. 2000; 7:19–26. [PubMed: 11029766]
13. Kawashima A, Tsugawa S, Boku A, Kobayashi M, Minamoto T, Nakanishi I. Expression of alphav integrin family in gastric carcinomas: increased alphavbeta6 is associated with lymph node metastasis. Pathol Res Pract. 2003; 199:57–64. [PubMed: 12747466]
14. Sato T, Konishi K, Maeda K, Yabushita K, Miwa A. Integrin alpha v, c-erbB2 and DNA ploidy in lung metastases from colorectal cancer. Hepatogastroenterology. 2003; 50:27–30. [PubMed: 12629984]
15. Markovic-Lipkovski J, Brasanac D, Muller GA, Muller CA. Cadherins and integrins in renal cell carcinoma: an immunohistochemical study. Tumori. 2001; 87:173–8. [PubMed: 11504373]
16. Cooper CR, Chay CH, Pienta KJ. The role of alpha(v)beta(3) in prostate cancer progression. Neoplasia. 2002; 4:191–4. [PubMed: 11988838]
17. Goldberg I, Davidson B, Reich R, Gotlieb WH, Ben-Baruch G, Bryne M. Alphav integrin expression is a novel marker of poor prognosis in advanced-stage ovarian carcinoma. Clin Cancer Res. 2001; 7:4073–9. [PubMed: 11751504]

18. Trikha M, Zhou Z, Nemeth JA, Chen Q, Sharp C, Emmell E. CNTO 95, a fully human monoclonal antibody that inhibits alphav integrins, has antitumor and antiangiogenic activity in vivo. Int J Cancer. 2004; 110:326–35. [PubMed: 15095296]
19. Chen Q, Manning CD, Millar H, McCabe FL, Ferrante C, Sharp C. CNTO 95, a fully human anti alphav integrin antibody, inhibits cell signaling, migration, invasion, and spontaneous metastasis of human breast cancer cells. Clin Exp Metastasis. 2008; 25:139–48. [PubMed: 18064530]
20. Mullamitha SA, Ton NC, Parker GJ, Jackson A, Julyan PJ, Roberts C. Phase I evaluation of a fully human anti-alphav integrin monoclonal antibody (CNTO 95) in patients with advanced solid tumors. Clin Cancer Res. 2007; 13:2128–35. [PubMed: 17404096]
21. Chu FM, Picus J, Fracasso PM, Dreicer R, Lang Z, Foster B. A phase 1, multicenter, open-label study of the safety of two dose levels of a human monoclonal antibody to human alpha(v) integrins, intetumumab, in combination with docetaxel and prednisone in patients with castrate-resistant metastatic prostate cancer. Invest New Drugs. 2011; 29:674–9. [PubMed: 20145975]
22. O'Day SJ, Pavlick AC, Albertini MR, Hamid O, Schalch H, Lang Z. Clinical and pharmacologic evaluation of two dose levels of intetumumab (CNTO 95) in patients with melanoma or angiosarcoma. Invest New Drugs. 2012; 30:1074–81. [PubMed: 21331745]
23. O'Day S, Pavlick A, Loquai C, Lawson D, Gutzmer R, Richards J. A randomised, phase II study of intetumumab, an anti-alphav-integrin mAb, alone and with dacarbazine in stage IV melanoma. Br J Cancer. 2011; 105:346–52. [PubMed: 21750555]
24. Martin GS. The road to Src. Oncogene. 2004; 23:7910–7. [PubMed: 15489909]
25. Thomas SM, Brugge JS. Cellular functions regulated by Src family kinases. Annu Rev Cell Dev Biol. 1997; 13:513–609. [PubMed: 9442882]
26. Irby RB, Yeatman TJ. Role of Src expression and activation in human cancer. Oncogene. 2000; 19:5636–42. [PubMed: 11114744]
27. Talamonti MS, Roh MS, Curley SA, Gallick GE. Increase in activity and level of pp60c-src in progressive stages of human colorectal cancer. J Clin Invest. 1993; 91:53–60. [PubMed: 7678609]
28. Lombardo LJ, Lee FY, Chen P, Norris D, Barrish JC, Behnia K. Discovery of N-(2-chloro-6-methyl- phenyl)-2-(6-(4-(2-hydroxyethyl)- piperazin-1-yl)-2-methylpyrimidin-4-ylamino)thiazole-5-carboxamide (BMS-354825), a dual Src/Abl kinase inhibitor with potent antitumor activity in preclinical assays. J Med Chem. 2004; 47:6658–61. [PubMed: 15615512]
29. Olivieri A, Manzione L. Dasatinib: a new step in molecular target therapy. Ann Oncol. 2007; 18(6):vi42–6. [PubMed: 17591830]
30. Playford MP, Schaller MD. The interplay between Src and integrins in normal and tumor biology. Oncogene. 2004; 23:7928–46. [PubMed: 15489911]
31. Mitra SK, Schlaepfer DD. Integrin-regulated FAK-Src signaling in normal and cancer cells. Curr Opin Cell Biol. 2006; 18:516–23. [PubMed: 16919435]
32. Tucker GC. Alpha v integrin inhibitors and cancer therapy. Curr Opin Investig Drugs. 2003; 4:722–31.
33. Gasparini G, Brooks PC, Biganzoli E, Vermeulen PB, Bonoldi E, Dirix LY. Vascular integrin alpha(v)beta3: a new prognostic indicator in breast cancer. Clin Cancer Res. 1998; 4:2625–34. [PubMed: 9829725]
34. Folkman J, Haudenschild C. Angiogenesis in vitro. Nature. 1980; 288:551–6. [PubMed: 6160403]
35. Desgrosellier JS, Cheresh DA. Integrins in cancer: biological implications and therapeutic opportunities. Nat Rev Cancer. 2010; 10:9–22. [PubMed: 20029421]
36. Mas-Moruno C, Rechenmacher F, Kessler H. Cilengitide: the first anti-angiogenic small molecule drug candidate design, synthesis and clinical evaluation. Anticancer Agents Med Chem. 2010; 10:753–68. [PubMed: 21269250]
37. Shannon KE, Keene JL, Settle SL, Duffin TD, Nickols MA, Westlin M. Anti-metastatic properties of RGD-peptidomimetic agents S137 and S247. Clin Exp Metastasis. 2004; 21:129–38. [PubMed: 15168730]
38. Zhao Y, Bachelier R, Treilleux I, Pujuguet P, Peyruchaud O, Baron R. Tumor alphavbeta3 integrin is a therapeutic target for breast cancer bone metastases. Cancer Res. 2007; 67:5821–30. [PubMed: 17575150]

39. Ning S, Nemeth JA, Hanson RL, Forsythe K, Knox SJ. Anti-integrin monoclonal antibody CNTO 95 enhances the therapeutic efficacy of fractionated radiation therapy in vivo. Mol Cancer Ther. 2008; 7:1569–78. [PubMed: 18566227]
40. Lee EC, Lotz MM, Steele GD Jr, Mercurio AM. The integrin alpha 6 beta 4 is a laminin receptor. J Cell Biol. 1992; 117:671–8. [PubMed: 1533398]
41. Monnier Y, Farmer P, Bieler G, Imaizumi N, Sengstag T, Alghisi GC. CYR61 and alphaVbeta5 integrin cooperate to promote invasion and metastasis of tumors growing in preirradiated stroma. Cancer Res. 2008; 68:7323–31. [PubMed: 18794119]
42. Desgrosellier JS, Barnes LA, Shields DJ, Huang M, Lau SK, Prevost N. An integrin alpha(v)beta(3)-c-Src oncogenic unit promotes anchorage-independence and tumor progression. Nat Med. 2009; 15:1163–9. [PubMed: 19734908]
43. Schwartz MA, Ginsberg MH. Networks and crosstalk: integrin signalling spreads. Nat Cell Biol. 2002; 4:E65–8. [PubMed: 11944032]
44. Giancotti FG, Ruoslahti E. Integrin signaling. Science. 1999; 285:1028–32. [PubMed: 10446041]
45. Alghisi GC, Ruegg C. Vascular integrins in tumor angiogenesis: mediators and therapeutic targets. Endothelium. 2006; 13:113–35. [PubMed: 16728329]
46. Bellis SL, Perrotta JA, Curtis MS, Turner CE. Adhesion of fibroblasts to fibronectin stimulates both serine and tyrosine phosphorylation of paxillin. Biochem J. 1997; 325(Pt 2):375–81. [PubMed: 9230116]
47. Turner CE. Paxillin interactions. J Cell Sci. 2000; 113(Pt 23):4139–40. [PubMed: 11069756]

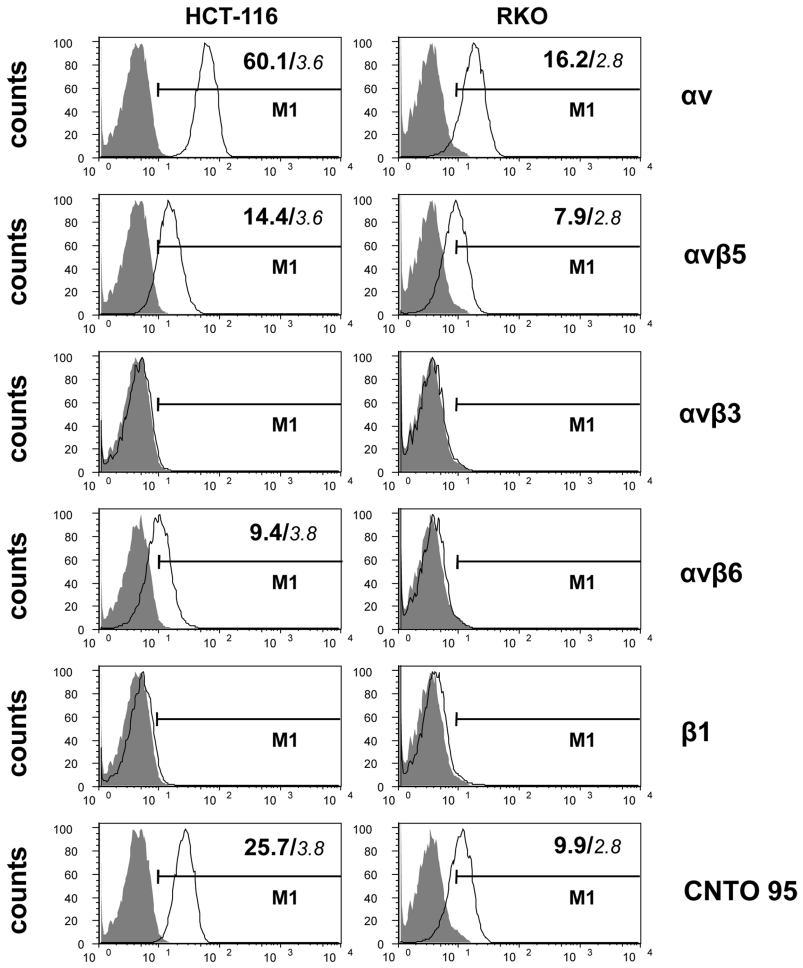

Figure 1. α_V integrin expression on HCT-116 cells and RKO cells by flow cytometry

Data were collected on 10,000 cells per sample and displayed as overlayed histograms depicting cell counts versus fluorescence intensity. A gate (M1) was set to exclude ~99% of isotype control cells (shade). The value of MFI was indicated in the upper right corner of the histogram for positively stained cells. Background MFI was calculated based on isotype control staining and was indicated in small Italic font. The Y axis represents the number of cells, the X axis represents the scale of fluorescent intensity of specific staining. The specific staining used in each row of histograms are indicated by the text on the right.

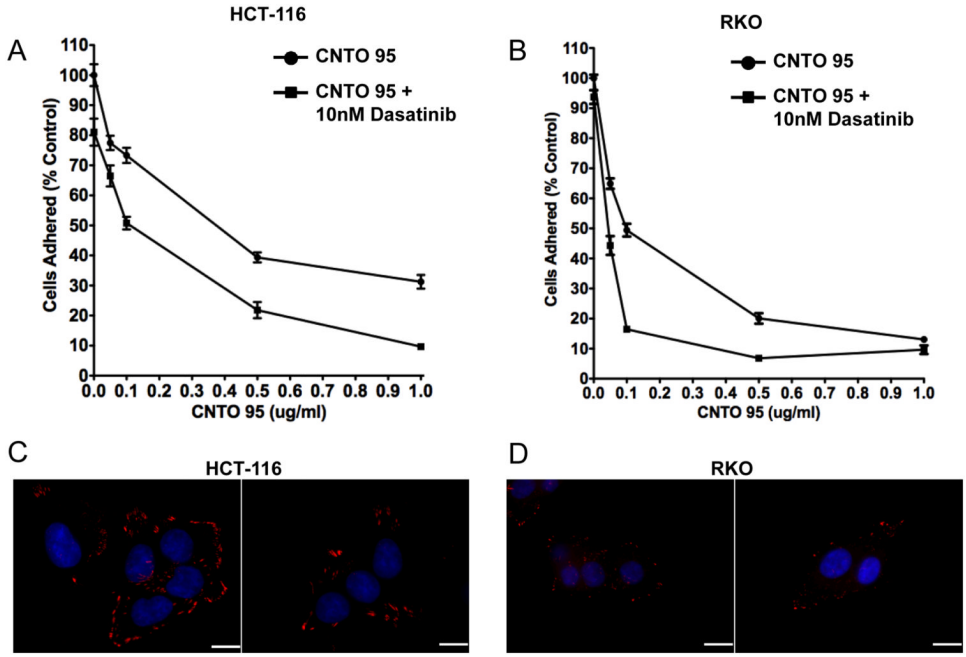

Figure 2. The effect of CNTO95 and dasatinib on the proliferation and survival of HCT-116 cells and RKO cells

The viability of HCT-116 cells (A) and RKO cells (B) was measured by MTS assays. Results are presented as the percent value of the untreated cells. Data are shown as the mean ± SE. The proliferation of HCT-116 cells (C) and RKO cells (D) were analyzed by flow cytometry. Data were collected on 50,000 cells per sample and displayed as overlayed histograms depicting cell counts versus CFSE fluorescence intensity. Cells that were not labeled with CFSE (gray shade) served as negative control for CFSE fluorescence background. The apoptosis and necrosis of HCT-116 cells (E) and RKO cells (G) were analyzed using annexin V and 7AAD staining by flow cytometry. Data were collected on 50,000 cells per sample and displayed as dot plots. Cells were pre-gated based on forward scatter and side scatter. Numbers in each quadrant represent the percentage of the total gated events. The apoptotic and necrotic cell death, as well as live cells in HCT-116 (F) and RKO (H) cell culture are quantified as bar graphs. Data were from 3 independent experiments and shown as the mean ± SD. *, significantly different from untreated cells, $P<0.05$.

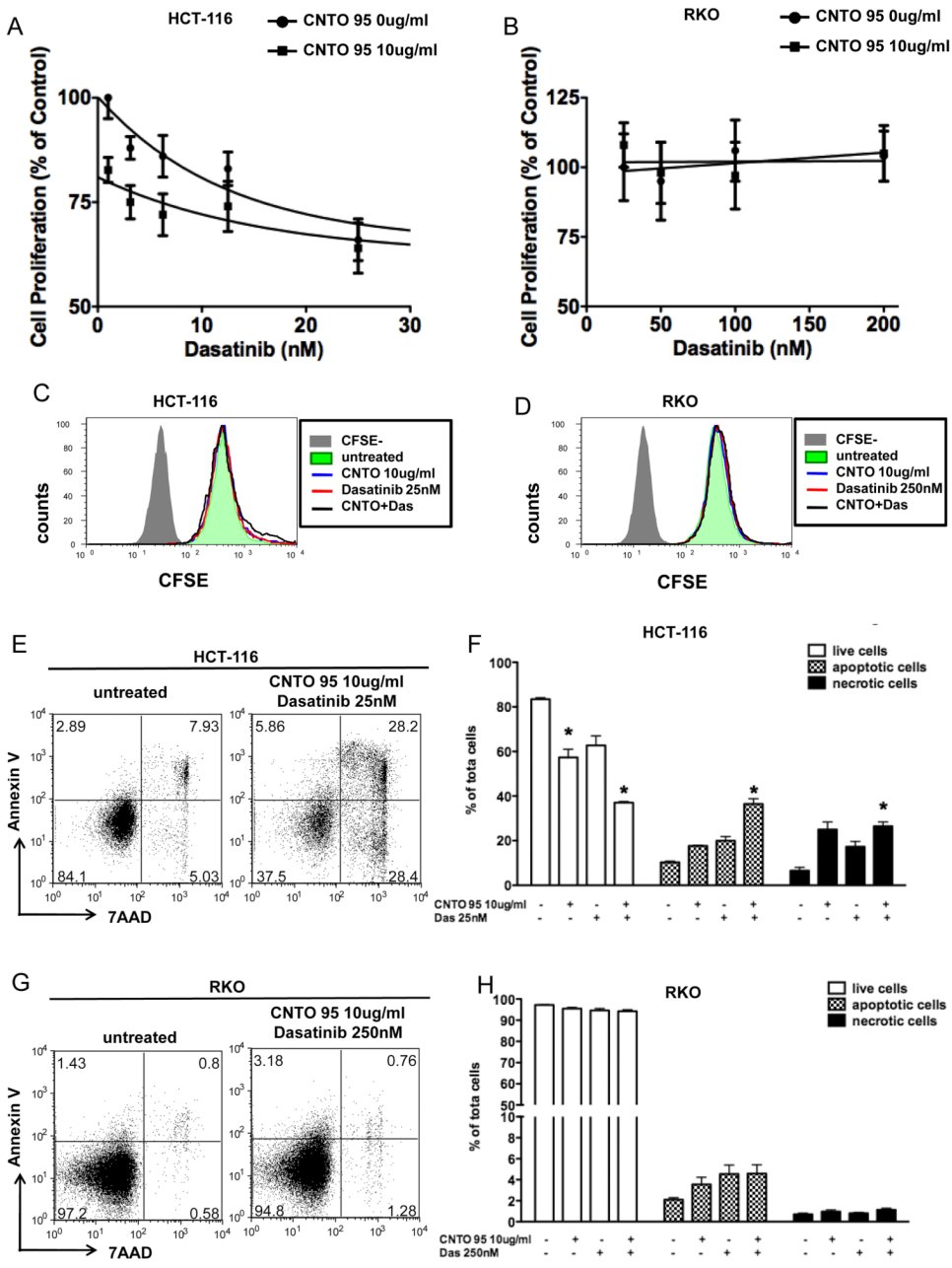

Figure 3. The effect of CNTO95 and dasatinib on the migration of HCT-116 cells (A-C) and RKO cells (D-F)

Cell migration upon exposure to various doses of CNTO95 (A, D) or dasatinib (B, E) as single agent treatment was assessed and depicted as percent value of the untreated cells. Quantifications of cell migration are displayed as bar graphs for HCT-116 cells (C) and RKO cells (F). *, significantly different from untreated control, $P<0.05$; **, significantly different from either drug treatment, $P<0.05$. Data are shown as the mean ± SD.

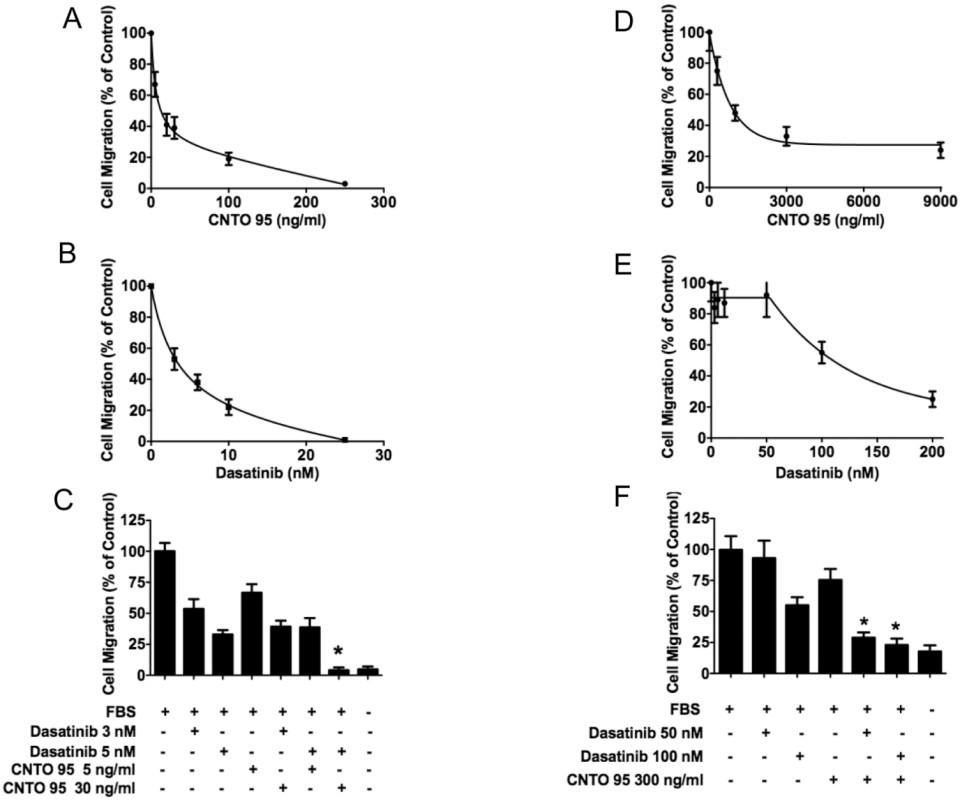

Figure 4. The effect of CNTO95 and dasatinib on HCT-116 cell and RKO cell adhesion

Adhesion to vitronectin of HCT-116 (A) and RKO (B) cells in the presence of CNTO95 and dasatinib. The number of adhered cells was quantified, and data shown as the mean ± SE. Levels of focal adhesion complexes in HCT-116 (C) and RKO (D) cells. Vinculin was visualized with an anti-vinculin anibody (red) and DNA was stained with DAPI (blue). Shown are two representative fields from each condition. Scale bar, 10uM.

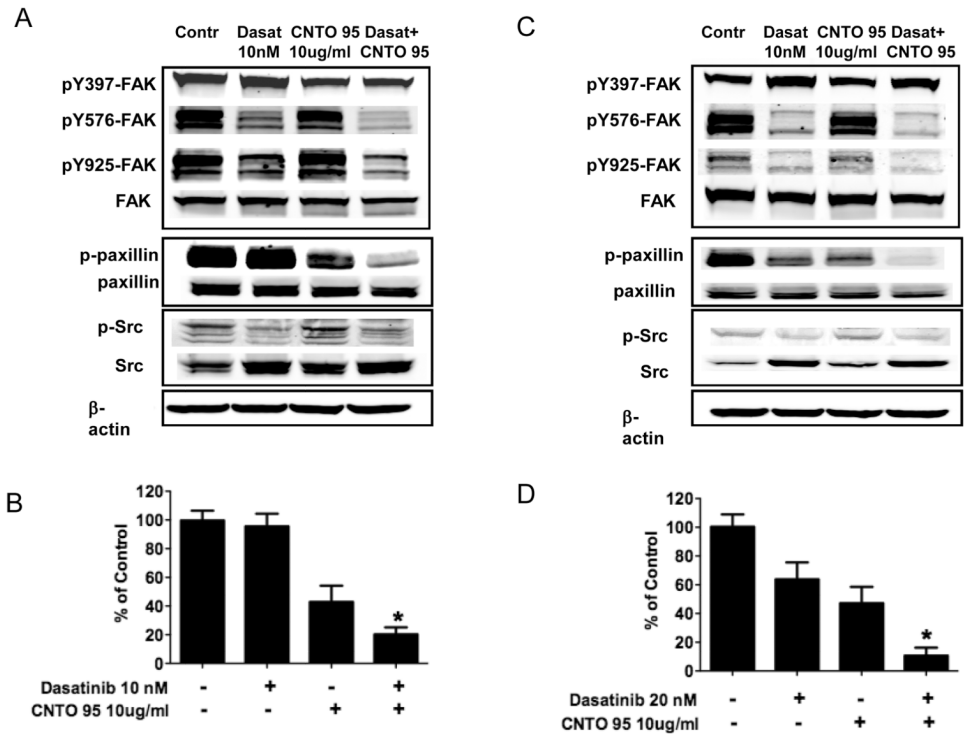

Figure 5. The effect of CNTO95 and dasatinib on integrin signal transduction in HCT-116 cells (A, B) and RKO cells (C, D)

Western blots of whole cell lysates from drug treated and untreated control HCT-116 cells (A) or RKO cells (C). Quantifications of paxillin phosphorylation in HCT-116 cells (B) and RKO cells (D) are displayed as bar graphs. *, significantly different from either drug treatment, $P<0.05$. Data are shown as the mean ± SD.

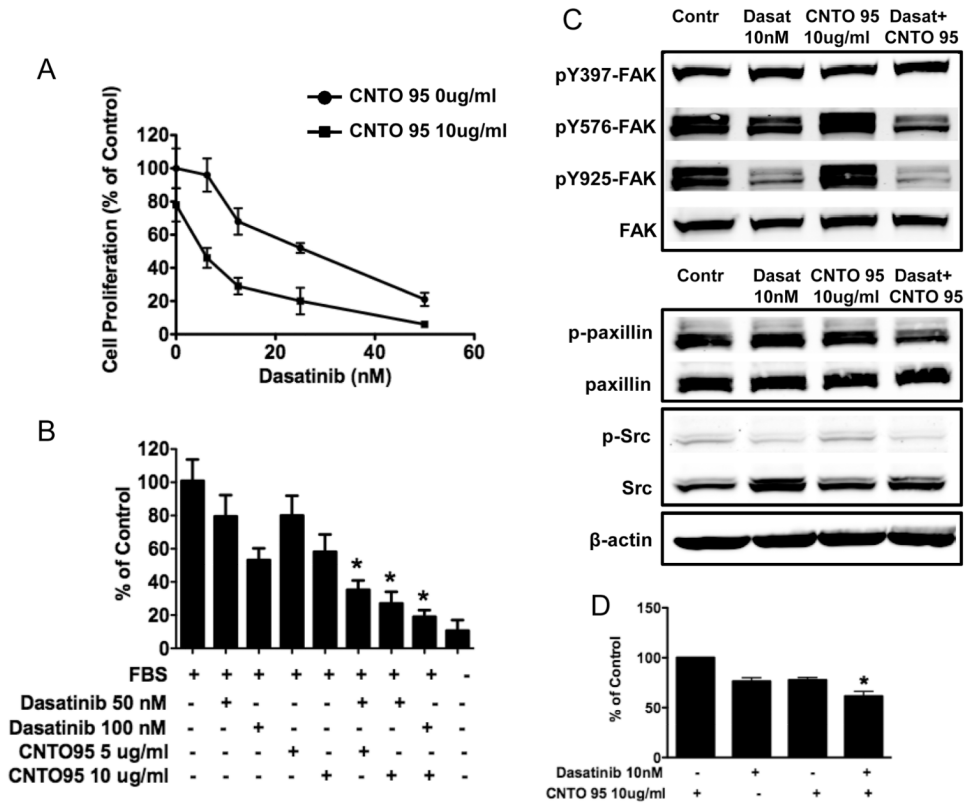

Figure 6. The effect of CNTO95 and dasatinib on HUVEC cell viability (A), invasion (B) and signal transduction (C, D)

(A) Inhibition of cell viability was presented as the percent value of the untreated cells. (B) Drug treatment induced inhibition on HUVEC cell invasion was quantified and displayed as the bar graph. (C) Western blots of whole cell lysates from drug treated and untreated HUVEC cells. (D) Drug treatment induced inhibition on paxillin phosphorylation was quantified and presented as the bar graph. *, significantly different from either drug treatment, $P<0.05$. Data are shown as the mean ± SD.

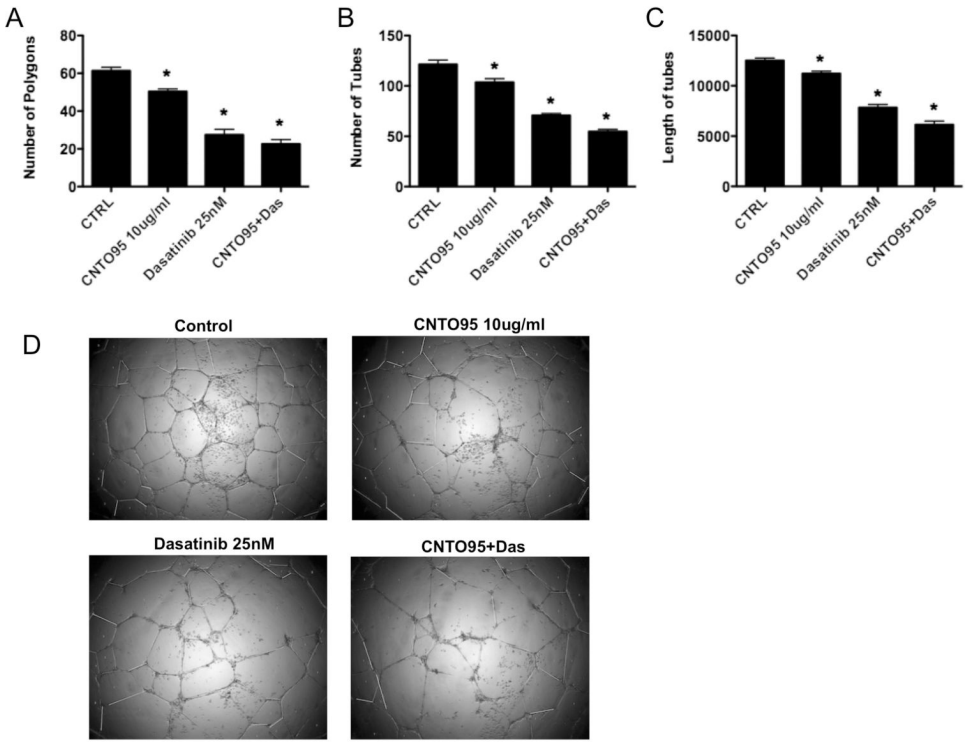

Figure 7. The effect of CNTO95 and dasatinib on HUVEC tubular network formation

Bar graphs showing quantitative comparison of (A) total numbers of closed polygons, (B) total number of tubes, and (C) length of aligned tubes among control and drug treated groups. Data are shown as the mean ± SD as representative of 3 independent assays. *, significantly different from untreated control, $P<0.05$. (D) Images of HUVEC tubular formation on matrigel. A representative field from each condition is shown.